NF-kappaB has a Major Role in Breast Cancer through activation of EMT-Transcription Factors, Immune Signaling and Redox Mechanisms

Bruno R. B. Pires[1,2] (DO); Renata Binato[1,2]; Gerson M. Ferreira[1,2]; Andre L. Mencalha[3]; Stephany Corrêa[1,2]; Carolina Panis[4] and Eliana Abdelhay[1,2]

1 Laboratório de Célula-Tronco, Divisão de Laboratórios do Centro de Transplante de Medula Óssea, Instituto Nacional de Câncer, Rio de Janeiro, RJ, Brazil;
2 Instituto Nacional de Ciência e Tecnologia para o Controle do Câncer, Brazil;
3 Departamento de Biofísica e Biometria, Universidade do Estado do Rio de Janeiro, Rio de Janeiro, RJ, Brazil; 4 Laboratório de Mediadores Inflamatórios, Universidade Estadual do Oeste do Paraná, Francisco Beltrão, PR, Brazil

ABSTRACT

Breast cancer (BC) is a heterogeneous disease composed of multiple subtypes with different molecular characteristics and clinical outcomes. In Brazil, this neoplasia is the first cause of cancer death in women, mainly due to the diagnosis in advanced stages, when the possibility of the development of metastasis is greater. The metastatic process in BC is related to the expression of the epithelial-to-mesenchymal transition transcription factors (EMT-TFs) SNAIL, SLUG, SIP1 and TWIST1. We examined the role of NF-κB in the aggressive properties and regulation of EMT-TFs in human BC cells. Blocking NF-κB/p65 activity by reducing its transcript and protein levels (through siRNA-strategy and dehydroxymethylepoxyquinomicin [DHMEQ] treatment) in the aggressive MDA-MB-231 (Triple Negative, TNBC) and HCC-1954 (HER2/neu positive) cell lines resulted in downregulation of SLUG, SIP1, TWIST1, MMP11 and N-cadherin and upregulation of E-cadherin transcripts. Bioinformatics tools identified several NF-κB binding sites along the promoter region of SNAIL, SLUG, SIP1 and TWIST1 genes, which were confirmed by chromatin immunoprecipitation and luciferase reporter assays. Thus, we suggest that NF-κB directly regulates the transcription of EMT-TF genes in breast cancer. Further, we evaluated the mRNA levels for NF-κB, Twist, Slug, and Sip1 on 46 breast tumor samples. Comparing the BC subtypes, we observed that TNBC expressed more Slug and Sip1 than other groups and, interestingly, Twist1 was overexpressed in HER2 samples. Twist1 is described to be the master regulator of EMT in BC, however, its role during the evolution of the intrinsic BC subtypes remains unclear. To investigate the biological significance of Twist1 for HER2 subtype, we silenced its expression using shRNA-approach in HCC-1954 cells. Compared to negative silencing control (Scramble), Twist1 knockdown resulted in 92% reduction of its mRNA levels. We also observed that the knockdown caused profound molecular alterations in Her2 cells, because a large-scale microarray analysis by GeneChip human exon array showed altered expression of 311 genes. Metacore software grouped these genes according to molecular function, revealing numerous correlations between Twist1 with important biological processes and signaling pathways such as Blood Coagulation, TGF-β/SMADs, Interleukin-17, and e.g. Together, our findings may contribute to a greater understanding of the metastatic process of this neoplasia and point out NF-κB and Twist1 as potential target for breast cancer treatment. Oxidative stress is a well-known condition to ensure the genomic instability, especially in BC, which redox alterations have been widely characterized. However, the molecular triggers have still to be identified. In this context, we have investigated the role of the main pro-oxidant transcription factor, NF-κB, in BC subtypes gene profile, using microarray approach. Our results showed that NF-κB knockdown in MDA-MB-231 (TNBC), HCC-1954 (HER2) and MCF-7 (Luminal) lead to differential expression of relevant members from glutathione metabolism, prostaglandins, cytochrome P450 and cyclooxygenase, suggesting a relation between redox balance and NF-κB in such cells. We also validated the microarray dataset focusing on oxidative stress, performing biochemical analyses regarding the antioxidant capacity, lipid peroxidation profile and nitric oxide status in BC cells. Our data showed a distinct pattern of the oxidative status in each one of the three studied cell lines, explained by the intrinsic characteristics of each BC subtype. Thus, our findings suggest that NF-κB may represent an additional mechanism related with oxidative stress maintenance in BC, operating by various forms to deal with other important predominant signaling for each BC subtype.

RESULTS

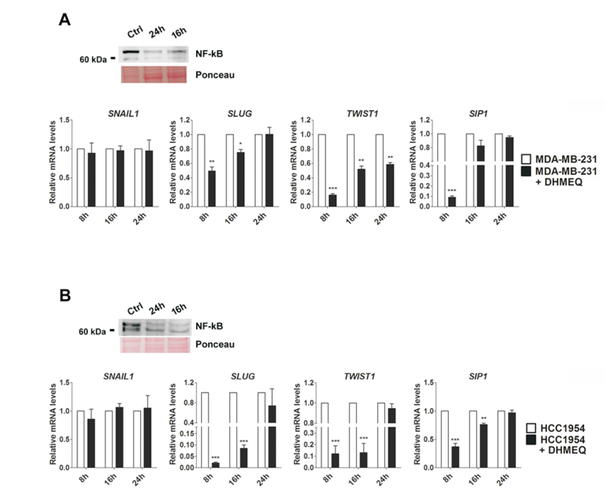

Figure 1. Relative expression of the EMT-inducing factors after NF-κB/p65 signaling inhibition. The mRNA levels of SNAIL1, SLUG, TWIST1, and SIP1 were assessed in MDA-MB-231 (A) and HCC-1954 (B) cells at 8, 16 and 24 h of DHMEQ treatment. NF-κB/p65 inhibition was evaluated at protein levels by western blot assay at 16 and 24 h of DHMEQ treatment. Ponceau staining was used as a loading control. Ctrl: control. DHMEQ: dehydroxymethylepoxyquinomicin. The data were expressed as the mean ± SD. * = p<0.05, ** = p<0.01, *** = p<0.001.

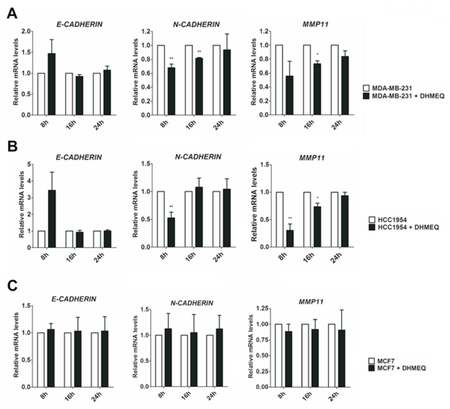

Figure 2. Relative expression of EMT-phenotype markers after NF-κB/p65 signaling inhibition. The mRNA levels of E-CADHERIN, N-CADHERIN and MMP11 were assessed in MDA-MB-231 (A) and HCC-1954 (B) cells at 8, 16 and 24 h of DHMEQ treatment. The data were expressed as the mean ± SD. * = p<0.05, ** = p<0.01, *** = p<0.001.

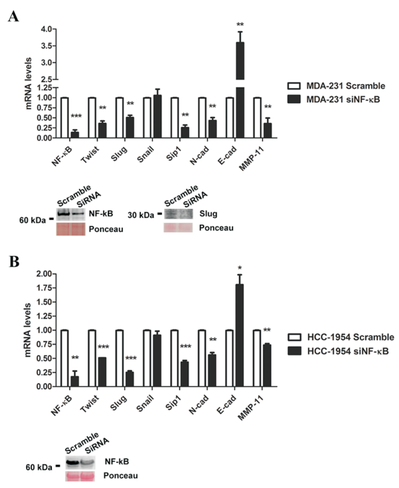

Figure 3. Relative expression of EMT-phenotype markers after NF-κB/p65 signaling inhibition. The mRNA levels of E-CADHERIN, N-CADHERIN and MMP11 were assessed in MDA-MB-231 (A) and HCC-1954 (B) cells at 8, 16 and 24 h of DHMEQ treatment. The data were expressed as the mean ± SD. * = p<0.05, ** = p<0.01, *** = p<0.001.

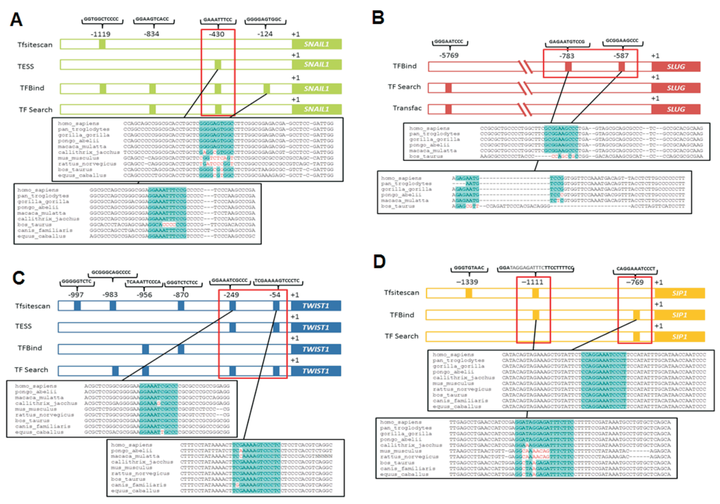

Figura 4. Representative scheme of putative NF-κB binding sites located in the SNAIL1 (A), SLUG (B), TWIST1 (C) and SIP1 (D) promoter regions predicted by Tfsitescan, TESS, TFBind, TFSearch and Transfac bioinformatics tools. An alignment of the DNA region showed evolutionarily conservation among metazoan species. Identical nucleotides are in the blue. Red boxes indicate the regions investigated by chromatin immunoprecipitation. +1: transcription start site.

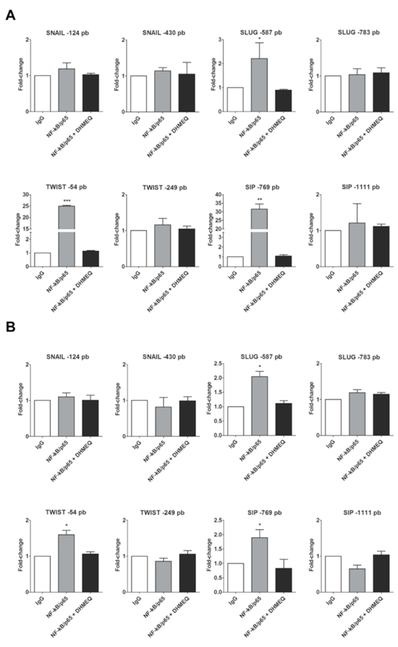

Figura 5. ChIP-qPCR of predicted NF-κB/p65 binding sites in the SNAIL1, SLUG, TWIST1 and SIP1 promoter regions using MDA-MB-231 (A) and HCC-1954 (B) cells. The histograms set a fold-change of each site by comparing the IgG negative control to NF-κB/p65 antibodies with the natural and treated with DHMEQ, the specific NF-kB/p65 inhibitor. DHMEQ: dehydroxymethylepoxyquinomicin. The data were expressed as the mean ± SD. * = p<0.05, ** = p<0.01, *** = p<0.001

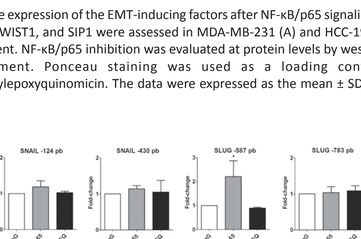

Figure 9. Silencing of Twist1 in Her2 breast cancer cells HCC-1954. Relative expression of Twist1 after its knockdown using shRNA-approach. (A). Hierarchical clustering of differentially expressed genes identified by chip array assay (B). The data were analyzed using Partek® software and 2-fold change was used as criteria to define up-regulation (red) or down-regulation (green). Scramble is the negative silencing control.

Figure 10. Biological process analysis of transcripts that have their expression up-regulated or down-regulated as a result of Twist1 silencing. The processes are arranged by Metacore software according to a statistical significance of the number of genes presented in each group.

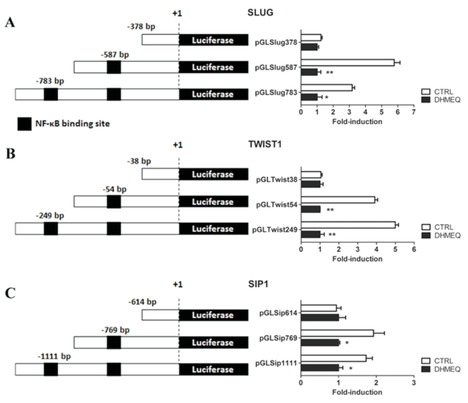

Figure 6. Relative luciferase activity in MDA-MB-231 cells transfected with pGL3-plasmid containing the SLUG (A), TWIST1 (B) and SIP1 (C) promoter regions. The firefly luciferase was normalized to the renilla vector, and the values are relative to the pGL3 (Mock) signal. The black boxes in the schematic plasmid constructs represent NF-κB binding sites. The bar graphs represent the relative luciferase activities of each construct in MDA-MB-231 cells. The white bars indicate natural NF-κB expression, and the black bars show NF-κB inhibition through DHMEQ treatment. DHMEQ: dehydroxymethylepoxyquinomicin, the specific NF-kB/p65 inhibitor. Each bar represents the mean ± SD.

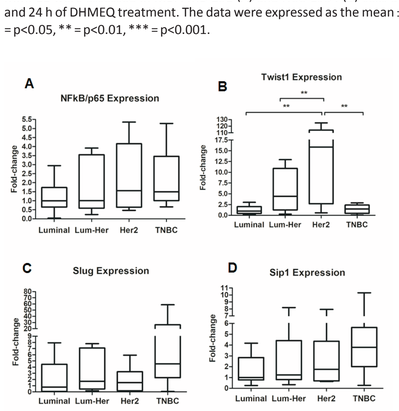

Figure 7. Box-plot graphs showing gene expression for NF-kB/p65 (A), Twist1 (B), Slug (C) and Sip1 (D) in Luminal (hormone receptor-positive ER and/or PR), HER-2 and Triple-negative (TNBC) breast cancer subtypes. Median and range of mRNA values are shown. Expression was normalized by ACTB and GAPDH mRNA levels and Ct was calculated vs. Luminal median. * = p<0.05 ** = p<0.01, *** = p<0.001.

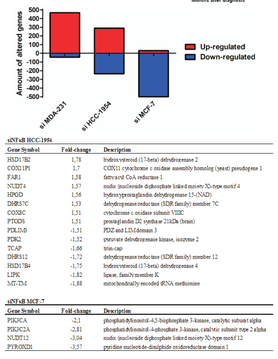

siNFκB HCC-1954

Gene Symbol	Fold-change	Description
HSD17B2	1,78	hydroxysteroid (17-beta) dehydrogenase 2
COX11P1	1,7	COX11 cytochrome c oxidase assembly homolog (yeast) pseudogene 1
FAR1	1,58	fatty-acid CoA reductase 1
NUDT4	1,57	nudix (nucleoside diphosphate linked moiety X)-type motif 4
HPGD	1,56	hydroxyprostaglandin dehydrogenase 15-(NAD)
DHRS7C	1,53	dehydrogenase/reductase (SDR family) member 7C
COX5C	1,51	cytochrome c oxidase subunit VIIIC
PTGDS	1,51	prostaglandin D2 synthase 21kDa (brain)
FDL1N	-1,51	FDZ and LDLdomain 3
PGK2	-1,52	pyruvate dehydrogenase kinase, isozyme 2
TCAP	-1,66	titin-cap
DHRS12	-1,72	dehydrogenase/reductase (SDR family) member 12
HSD17B4	-1,75	hydroxysteroid (17-beta) dehydrogenase 4
LIPE	-1,82	lipase, family member E
MT-TM	-1,88	mitochondrially encoded tRNA methionine

siNFκB MCF-7

Gene Symbol	Fold-change	Description
PIK3CA	-2,1	phosphatidylinositol-4,5-bisphosphate 3-kinase, catalytic subunit alpha
PIK3CA	-2,81	phosphatidylinositol-4-phosphate 3-kinase, catalytic subunit type 2 alpha
NUDT12	-3,04	nudix (nucleoside diphosphate linked moiety X)-type motif 12
PYROXD1	-3,57	pyridine nucleotide-disulphide oxidoreductase domain 1

siNFκB MDA-MB-231

Gene Symbol	Fold-change	Description
ALDH3A1	25,9	aldehyde dehydrogenase 1 family, member A3
AKR1B10	21,19	aldo-keto reductase family 1, member B10 (aldose reductase)
DHRS9	10,72	dehydrogenase/reductase (SDR family) member 9
PTGES	9,4	prostaglandin E synthase
DHRS3	8,23	dehydrogenase/reductase (SDR family) member 3
RDH10	7,02	retinol dehydrogenase 10 (all-trans)
GPX2	5,01	glutathione peroxidase 2 (gastrointestinal)
PTGS2	5,01	prostaglandin-endoperoxide synthase 2 (prostaglandin G/H synthase and cyclooxygenase)
PTGFRN	4,57	prostaglandin F2 receptor inhibitor
AKR1C2	3,5	aldo-keto reductase family 1, member C2; aldo-keto reductase family 1 member C2-like
STS	3,48	steroid sulfatase (microsomal), isozyme S
GSTT1	3,42	glutathione S-transferase theta 1
MAOA	3,13	monoamine oxidase A
CYP4B1	3,05	cytochrome P450, family 4, subfamily B, polypeptide 1
PIK3C2B	2,92	phosphatidylinositol-4-phosphate 3-kinase, catalytic subunit type 2 beta
CP	2,78	ceruloplasmin (ferroxidase)
SQRDL	2,62	sulfide quinone reductase-like (yeast)
CYB5A	2,52	cytochrome b5 type A (microsomal)
SEPW1	2,39	selenoprotein W, 1
IDO1	2,38	indoleamine 2,3-dioxygenase 1
NDUFB9	2,36	NADH dehydrogenase (ubiquinone) 1 beta subcomplex, 9, 22kDa
SRD5A3	2,35	steroid-5-alpha-reductase 3
BLVRB	2,21	biliverdin reductase B (flavin reductase (NADPH))
NDUFS6	2,18	NADH dehydrogenase (ubiquinone) Fe-S protein 6, 13kDa (NADH-coenzyme Q reductase)
PTGER4	2,16	prostaglandin E receptor 4 (subtype EP4)
IDH1	2,13	isocitrate dehydrogenase 1 (NADP+), soluble
UQCRB	2,13	ubiquinol-cytochrome c reductase binding protein
BCKDHA	2,06	branched chain keto acid dehydrogenase E1, alpha polypeptide
HPGD	2,06	hydroxyprostaglandin dehydrogenase 15-(NAD)
PIP4K2C	2,06	phosphatidylinositol-5-phosphate 4-kinase, type II, gamma
OCLC	2,05	glutamate-cysteine ligase, catalytic subunit
XDH	2,04	xanthine dehydrogenase
DHRS3R1	2,02	dihydroorotate dehydrogenase (quinone)
PITPNC1	2,01	phosphatidylinositol transfer protein, cytoplasmic 1
GSTM3	-2,56	glutathione S-transferase mu 1

Figure 12. Differentially expressed genes identified by chiparray assay showing increased and decreased genes in NF-κB-silenced breast cancer cell lines compared with scramble counterpart, and list of stress oxidative associated-genes with altered expression in consequence of the knockdown.

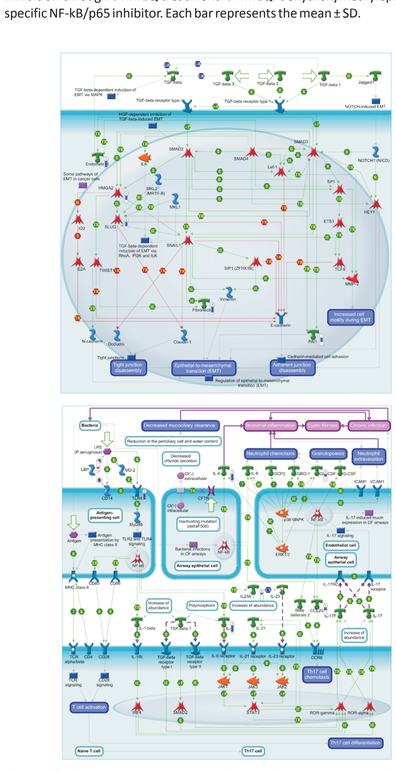

Figure 11. Pathway maps of the main signaling altered according to the statistical significance (p-value) of the gene distribution in the analyzes. (A) *Epithelial-to-Mesenchymal Transition dependent on TGF-ß /SMADs* was the main signaling altered as a result of Twist1 silencing. (B) *Th17-mediated Immune Response* was the second signaling more altered in consequence of Twist1 silencing. . The relative expression data of the genes identified in the study are visualized on the map through a thermometer in blue (for down-regulation) or red (for up-regularion).

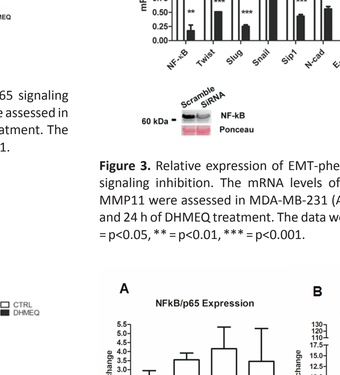

Figure 13. Thiol content. MCF-7 (A and B), HCC (C and D) and MDA-MB231 (E and F) cells treated (DHMEQ column) or not (CTR column) with the NF-κB inhibitor for 24 or 48 hours. Data are expressed as means and standard errors of the means. * indicates statistical significance (p<0.05).

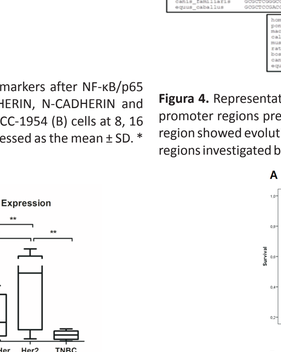

Figure 14. Lipid peroxidation profile. MCF-7 (A and B), HCC (C and D) and MDA-MB231 (E and F) cells treated (DHMEQ) or not (CTR) with the NF-κB inhibitor for 24 or 48 hours. Data are expressed as means. * indicates statistical significance (p<0.05).

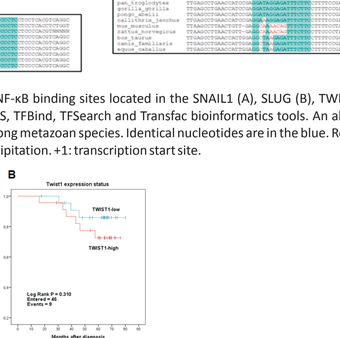

Figure 15. Nitrite as estimative of NO levels. MCF-7 (A and B), HCC (C and D) and MDA-MB231 (E and F) cells treated (DHMEQ column) or not (CTR column) with the NF-κB inhibitor for 24 or 48 hours. Data are expressed as means and standard errors of the means. * indicates statistical significance (p<0.05).

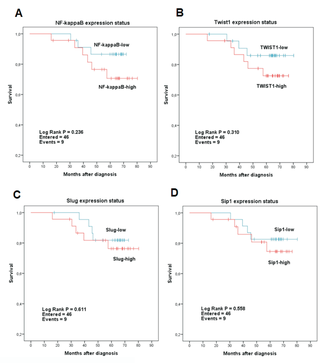

Figure 8. Kaplan-Meier's survival analysis in breast cancer patients according to the expression of NF-κB/p65 (A), Twist1 (B), Slug (C) and Sip1 (D).

Projeto Gráfico: Serviço de Edição e Informação Técnico-Científica / INCA